H IGHLY SELECTIVE H_2 SEPARATION ZEOLITE MEMBRANES FOR COAL GASIFICATION MEMBRANE REACTOR APPLICATIONS

Annual Technical Progress Report

Reporting Period:

September 2004 – September 2005

DOE Award No. DE-FG26-02NT41536

Mei Hong (student), Richard D. Noble* (PI) and John L. Falconer (co-PI)

University of Colorado

Department of Chemical and Biological Engineering

Boulder, Colorado 80309-0424

Phone: (303) 492 6100; Fax: (303) 492 4341; Email: Nobler@Colorado.edu

December 12, 2005

ABSTRACT

Zeolite membranes are thermally, chemically, and mechanically stable. They also have tunable molecular sieving and catalytic ability. These unique properties make zeolite membrane an excellent candidate for use in catalytic membrane reactor applications related to coal conversion and gasification, which need high temperature and high pressure range separation in chemically challenging environment where existing technologies are inefficient or unable to operate. Small pore, good quality, and thin zeolite membranes are needed for highly selective H_2 separation from other light gases (CO_2, CH_4, CO).

In an effort to develop zeolite membranes more suitable for H_2 separation, various types of thin zeolite membranes were modified. The aim of the modification is to tune the size of zeolite pores and/or to decrease the number of defects within as-synthesized zeolite membranes. The modification attempts include silylation on medium-pore MFI (Al-ZSM-5 and B-ZSM-5) and small-pore CHA (SAPO-34) membranes, and ion exchange on SAPO-34 membranes. Silylation on MFI membranes can reduce the medium zeolite pores and increase H_2 selectivity both in single component and in mixtures with CO_2, CH_4, or N_2. For example, for one B-ZSM-5 membrane after silylation, the H_2/CO_2 separation selectivity at 473 K increased from 1.4 to 37, whereas the H_2/CH_4 separation selectivity increased from 1.6 to 33. The H_2 permeance and H_2/CO_2 and H_2/CH_4 separation selectivities increased with temperature. At 673 K, the H_2 permeance was 1.0×10^{-7} $mol\cdot m^{-2}\cdot s^{-1}\cdot Pa^{-1}$, and the H_2/CO_2 separation selectivity was 47. Above 673 K, the silylated membrane catalyzed reverse water gas shift reaction but still could separate H_2 with high selectivity; and thermally stable. However, silylation decreased H_2 permeance more than one order of magnitude in the B-ZSM-5 membrane. The silylation results on MFI membranes depended on the initial membrane quality and acidity. Different silane precursors did not yield significant different H_2 separation performance. Silylation on CHA membranes blocked defects within the membranes; it increased H_2/CH_4 and CO_2/CH_4 selectivities but did not increase H_2/CO_2 and H_2/N_2 selectivities. Ion exchange of SAPO-34 membranes from H^+ form to Cu^{2+} or K^+ form was conducted. The H_2 selectivity did not show significant increase, but the CO_2/CH_4 selectivity increased ~ 50%.

This is the third annual technical progress report for the university coal research program supported by U.S. DOE NETL (Contract No. DE-FG26-02NT41536). This report summarizes program accomplishments up to December 2005. The report includes an introduction summarizing the research objectives and tasks; it also provides a summary of program activities and accomplishments covering progress in various zeolite membrane synthesis and modification. Possible future work is proposed as well.

TABLE OF CONTENTS

LIST OF FIGURES

LIST OF TABLES

1. INTRODUCTION

Hydrogen, as a clean energy source, is in increasing demand in industry. Hydrogen can be produced from coal conversion and gasification process where coal is converted into synthesis gas. Depending on the particular gasification process, the synthesis gas produced also contains carbon dioxide, methane, carbon monoxide, hydrogen sulfide, water, and other gases. Hydrogen recovery from coal gasification products requires an efficient separation process to purify the gas economically. Traditional separation methods, such as absorption, adsorption and distillation require pressure swings and/or changes in temperature. They are energy intensive and too expensive to purify dilute H_2. On the other hand, membrane processes are considered to be one of the most promising technologies for generation of pure hydrogen, taking advantage of continuous low energy operation.

Inorganic zeolite membranes have the ability to operate the separation at or near the processing conditions for H_2 production. They can tolerate high temperatures, high pressure-drops and chemically challenging environments. A zeolite layer can be fabricated onto a tubular support, providing high surface to volume ratio, scale up in modular form and the ability to continuously separate. Moreover, zeolites have catalytic properties, which make it possible to integrate reaction and separation into one unit. However, currently used zeolite membranes have not been successful for H_2 separation. This is mainly because the as-synthesized zeolite membranes either have zeolite pores too big for separating H_2 from other light gases or have many non-zeolite pores bigger than the zeolite pores, so called defects. Zeolite membranes with smaller pores should have the potential to effectively separate H_2 from other light gases, if they are made defect-free.

Zeolites are microporous crystalline alumino-silicates, with uniform pores in the molecular size range; the pore size distribution is extremely narrow. Most zeolites contain Si and Al, but other metals (B, Fe, and Ge) can be isomorphously substituted in some framework instead of Al and some frameworks can be prepared in the pure Si form. To selectively separate H_2 from other light gases (CO, CO_2, CH_4), the zeolite membrane will have to discriminate between molecules that are approximately 0.3-0.4 nm in size and 0.1 nm or less in size difference. The zeolite membranes need to have small pores and negligible amount of defects to ensure high selectivity. They also need to be thin to ensure high flux. To accomplish this goal, we can either synthesize small pore zeolite membranes that have pores in this size range, or post-treat existing zeolite membranes to systematically reduce the pore size and/or the number of defects so as to create good-quality zeolite membranes with desirable pore diameters suitable for hydrogen separation.

Among various types of zeolite membranes synthesized to date, ten-member ring MFI structure (silicalite-1 and ZSM-5) is the most extensively studied case. MFI type membranes have straight, circular channels of 0.54×0.56 nm running perpendicular to sinusoidal, elliptical channels of 0.51×0.54 nm, and are suitable for separations of several industrially important organic molecules. Light gas including H_2 separations, however, are often dominated by competitive adsorption, rather than size exclusion because the MFI pore size is much bigger than the size of light gases. The as-synthesized MFI membranes are sometimes selective towards CO_2 and CH_4, although H_2 is the smallest molecule because the adsorption of CO_2 and CH_4 is stronger than that of H_2, especially at low temperatures. Small pore zeolite membranes have been synthesized, which include zeolite A, SAPO-34, ETS-4, SSZ-13 and sodalite membranes. Our group has successfully synthesized SAPO-34 membranes, which have 8-member ring chabazite structure with pore size of 0.38 nm. The membranes showed high CO_2/CH_4 selectivities at low temperature range, but still have bigger non-zeolite defects in the structure.

In this report, we used two different approaches to post-treat as-synthesized zeolite membranes to alter their zeolite pore size and defects size: silylation and ion exchange. In the silylation reaction, silane precursor was firstly chemisorbed onto the acid sites within the zeolite membrane, then catalytically cracked on sites and oxidized. As a result, additional silicon atoms were added to the original zeolite structures, and the effective pore opening size of the defects and/or zeolite pores was decreased. In the ion exchange reaction, part of H^+ ions in the zeolite membranes was replaced by other metal cations. As a result, zeolite adsorption and/or diffusion properties changed, causing changes of the membrane permeation and separation properties. The effects of initial membrane properties and the modification parameters were studied in detail.

2. EXPERIMENTAL METHODS

2.1 Zeolite membrane synthesis

2.1.1 MFI membranes

Zeolite membranes with MFI structure have been prepared using difference synthesis procedures: secondary growth, vapor phase transport, and in-situ crystallization. The MFI membranes synthesized in this study were all prepared on the inner surface of porous (200-nm pores in inner layer; 0.35 porosity), tubular, asymmetric α-alumina supports (Pall Corporation).

Different types of 10-member ring MFI membranes were synthesized: Al-ZSM-5, B-ZSM-5 (Si/B=12.5 in the gel), B-ZSM-5 (Si/B=100 in the gel), and silicalite-1 membranes. Al-ZSM-5 membranes were synthesized with a standard in-situ crystallization procedure using NaOH in the gel. The gel composition is 2.0 TPABr : 19.46 SiO_2 : 0.389 $Al_2(SO_4)_3$: 500 H_2O : 2.5 NaOH, corresponding to a Si/Al ratio of 25. Sodium silicate was used as the silicon source, aluminum sulfate as the aluminum source, and tetra-propyl ammonium bromide (TPABr) as the template. Since the as-synthesized Al-ZSM-5 membranes were prepared in their Na^+ form, they need to be converted to their H^+ form before silylation. The Al-ZSM-5 membranes were ion exchanged to their H^+ form by a conventional ion exchange technique. The membranes were rotated in 1 M NH_4Cl solution at 368 K for 2 h and then heated to 503 K for 4 h.

Three types of boron substituted ZSM-5 (B-ZSM-5) membranes were synthesized. The first type of B-ZSM-5 membranes was synthesized by secondary growth on the inner surface of tubular α-alumina supports. Silicalite-1 seeds were made from a gel with a molar composition of 9 TPAOH : 24 SiO_2 : 500 H_2O : 96 EtOH, where tetra-propyl ammonium hydroxide (TPAOH) was used as the template, and tetraethoxysilane (TEOS) was used as the silicon source. The seeds were synthesized at 358 K for 3 days. The α-alumina supports were dip-coated three times with a suspension of silicalite-1 seeds (2 wt.% seeds in DI water). The secondary growth gel had a molar composition of 16 TPAOH : 80 SiO_2 : 6.5 $B(OH)_3$: 5000 H_2O : 320 EtOH, corresponding to a Si/B ratio of 12.5. In an attempt to minimize penetration into the support, the gel viscosity was increased by adding surfactant cetyltrimethyl ammonium bromide to the gel. Crystallization was carried out at 458 K for 4 h. An additional layer was applied using the same procedure, and the membranes were prepared with two layers. The thickness of a similar membrane broken and analyzed using scanning electron microscopy (SEM) (ISI SX-30, at 30 keV) was approximately 3.5 µm. The inverted pyramid shape of the zeolite crystals suggests c-orientation of the zeolite layer.

The second type of B-ZSM-5 membranes was synthesized by vapor phase transport method. The parent gel had a molar composition of 5 TPAOH : 12.5 TEOS : 1 $B(OH)_3$: 45 H_2O, also corresponding to a Si/B ratio of 12.5. The parent gel was aged at 353 K for 3 days. The supports were dipped in the parent gel and dried. A solution of 7 wt% TPAOH in water was added to the bottom of the support inside as the vapor source. The borosilicate dry gel was crystallized in the mixed vapor of TPAOH and water under autogenous pressure at 443 K for 20 h in an autoclave. A similar membrane was broken and analyzed using SEM. It does not have a uniform layer, the zeolite penetrated approximately 50 µm inside the support, and the average crystal size was 2.5 µm.

The third type of B-ZSM-5 membrane was synthesized in-situ from a gel with Si/B ratio of 100. The gel composition was 1.5 TPAOH : 19.5 SiO_2 : 0.195 $B(OH)_3$: 438H_2O, where colloidal silica was used as the silicon source and boric acid was used as the boron source. Crystallization was carried out at 458 K for 24 h. Additional layers were applied using the same procedure at 458 K for 48 h, and the membrane was prepared with 4 layers. The membrane were 85-100 µm thick and composed of randomly oriented crystals 5-10 µm in diameter.

Silicalite-1 membrane was also prepared in-situ using the gel of 1.5TPAOH: 19.5SiO_2: 438H_2O, and the silicon source was also colloidal silica. The synthesis procedure was the same as for B-ZSM-5 membranes with a Si/B ratio of 100. The silicalite-1 membrane was also prepared with 4 layers.

After crystallization, all the MFI membranes were impermeable to N_2 for a 138-kPa pressure drop at room temperature. They were calcined at 753 K for 8 h to remove the TPAOH template from the framework with a heating and cooling rate of 0.6 and 0.9 K/min respectively. Table 1 shows the synthesis conditions and modification conditions for different MFI membranes discussed in this report.

Table 1. Synthesis and silylation conditions for different MFI membranes

Membrane Number	Zeolite Type	Synthesis Method	Si/B	Silane precursor
A1	Al-ZSM-5	In-situ crystallization	25	MDES
B1-4, B6	B-ZSM-5	Secondary growth	12.5	MDES
B5	B-ZSM-5	Vapor phase transport	12.5	MDES
B7	B-ZSM-5	In-situ crystallization	100	MDES
B8	B-ZSM-5	Secondary growth	12.5	Diluted silane
Silicalite-1	Silicalite-1	In-situ crystallization	Infinity	MDES

2.1.2 CHA membranes

One kind of 8-member ring CHA membrane was prepared: SAPO-34 membrane. The SAPO-34 membranes were prepared by in-situ crystallization onto tubular stainless steel supports (0.8-µm pores, Pall Corp.). The synthesis gel had a molar composition of Al_2O_3 : P_2O_5: 0.6 SiO_2: 1.07 TEAOH: 56 H_2O. The gel was prepared by stirring H_3PO_4 (85 wt% aqueous solution), Al(i-

$C_3H_7O)_3$, and H_2O at room temperature for 12 h. The template, tetra-ethyl ammonium hydroxide (TEAOH, 35 wt% aqueous solution), was then added and the mixture was stirred for 30 min before the colloidal silica sol (Ludox AS40) was added. The porous stainless steel support was placed in an autoclave with synthesis gel both inside and outside the support tube. The hydrothermal synthesis was carried out at 468 K for 20 h. After synthesis, the membrane was washed with distilled water at room temperature and dried at 373 K in a vacuum oven for 2 h. Additional layers were applied using the same procedure, and membranes were prepared with 4 layers. The SAPO-34 membranes were calcined in air at 663 K for 20 h with heating and cooling rates of 0.6 and 0.9 K/min respectively and stored in a 373 K oven until usage.

2.2 Silylation on zeolite membranes

For silylation with methyldiethoxysilane (MDES), the zeolite membranes were first outgassed in N_2 (UHP grade, Airgas) flow at 623 K overnight. Then N_2 bubbled through liquid methyldiethoxysilane (97+%, Alfa Aesar) at 297 K and flowed through the inside of the membrane tubes at 623 K for 10 h. After that, the membrane inside was then flushed with N_2, heated to 823 K with a heating rate of 0.6 K/min in air (breathing quality, Airgas) for 4 h, and cooled down in flowing N_2 at a rate of 1.1 K/min. The outgas-silylation-calcination cycle was repeated once. The same silylation procedures were used for SAPO-34 membranes except that the oxidation step was at 663 K and the oxidation time was extended to about 20 h.

For silylation of MFI membranes with silane (SiH_4), the membrane was first outgassed in N_2 flow at 623 K. Then diluted silane (8000 ppm in N_2) flowed through the inside of the membrane tube at 473 K for 48 h. The membranes were then oxidized with water at 473 K for 24 h and dried at 473 K under vacuum. The outgas-silylation-oxidization cycle was repeated once. The silane precursors used for different membranes are also summarized in Table 1.

2.3 Ion exchange on SAPO-34 membranes

The as-synthesized SAPO-34 membranes have negatively charged framework structure, and H^+ ions were present in the extra framework for charge neutralization. The H^+ ions in the SAPO-34 membranes were exchanged with Cu^{2+} and K^+ ions. Solutions containing Cu^{2+} or K^+ ions were prepared by dissolving copper acetate in methanol or potassium acetate in ethanol respectively. The membranes were stirred at 200 rpm in the 0.01 M Cu^{2+} at 328 K fro 4 h, or in 0.01 M K^+ at 348 K for 4 h, and calcined at 673 K for 2-3 h. The same procedure was repeated for complete exchange with the designated ions.

2.4 Membrane Permeation

Single-gas permeance through the membrane was measured in a dead-end stainless steel module at 295 and 473 K. The pressure difference across the membrane was 138 kPa, and the permeate side pressure was 84 kPa. Permeation rates were measured at room temperature using a 1-10-100 ml soap film flowmeter. The estimated permeance error was 2% if the gas permeance was between 10^{-5} to 10^{-9} $mol{\cdot}m^{-2}{\cdot}s^{-1}{\cdot}Pa^{-1}$. For gas permeance below 10^{-9} $mol{\cdot}m^{-2}{\cdot}s^{-1}{\cdot}Pa^{-1}$, the permeance error could be as high as 20%. The lowest measurable flow rate is estimated to be $7{\times}10^{-11}$ $mol{\cdot}m^{-2}{\cdot}s^{-1}{\cdot}Pa^{-1}$. Ideal selectivity is the ratio of single-gas permeances.

2.5 Membrane Separation

Hexane isomers were separated by vapor permeation in a continuous flow. A syringe pump introduced a 50/50 n-hexane/2,2-dimethylbutane (DMB) liquid feed into a preheated helium carrier flow (0.83 mL/s) where the liquid feed vaporized. The total organic feed concentration was maintained at 8%. Both sides of the membrane were at approximately 84 kPa, and a helium sweep gas (0.83 mL/s) was used on the permeate side. Feed, retentate, and permeate flow rates were controlled with mass flow controllers and measured with a soap film flowmeter. The vapor compositions were analyzed on-line by a HP 6890 GC with a flame ionization detector. Log-mean partial pressure differences were used to calculate the permeances. Separation selectivity is defined as the ratio of permeances.

Fifty/fifty gas mixtures of H_2/CO_2, H_2/CH_4, H_2/N_2, and CO_2/CH_4 were separated in a continuous flow system. The permeate pressure was 84 kPa, and the transmembrane pressure drop was 138 kPa. No sweep gas was used. Between 298 and 473 K, silicone O-rings were used to seal the membrane in the module; above 473 K, graphite ferrules were used. Steady state separations at 473 K were compared for these two sealing modes, and the variations in the permeances and selectivities for the two arrangements were within 2%. Feed, retentate, and permeate flow rates were measured with a soap film flowmeter, and compositions were analyzed on-line by a HP 5890 GC with a thermal conductivity detector. Gas permeances and separation selectivities were calculated in the same way as those for vapor permeation experiments.

2.6 Powder adsorption and structure study

B-ZSM-5 powder was synthesized by secondary growth method, similar to membrane B1-4, B6, and B7. Silicalite-1 seeds were made from a gel with a molar composition of 9 TPAOH : 24 SiO_2 : 500 H_2O : 96 EtOH, where tetra-propyl ammonium hydroxide (TPAOH) was used as the template, and tetraethoxysilane (TEOS) was used as the silicon source. The seeds were synthesized at 358 K for 3 days. The seed suspension were repeatedly centrifuged at 15,000 rpm and decanted until the pH of the suspension was below 8. The cleaned seeds were dried at 373 K overnight in a vacuum oven. The silicalite-1 seeds were hydrothermally grown in the presence of a secondary growth gel at 458 K for 4 h under horizontal rotation at ~ 60 rpm. The secondary growth gel had a molar composition of 16 TPAOH : 80 SiO_2 : 6.5 $B(OH)_3$: 5000 H_2O : 320 EtOH, corresponding to a Si/B ratio of 12.5. The B-ZSM-5 powder suspension was cleaned by repeated centrifugation at 2700 rpm and decanting. The cleaned B-ZSM-5 powder was calcined at 753 K for 8 h. Some calcined B-ZSM-5 powder was silylated with methyldiethoxysilane using the same method as for B-ZSM-5 membrane silylation. The silylation procedure was also repeated once for B-ZSM-5 powder.

The synthesized and silylated powder was used for gas adsorption in an Autosorb-1 (Quantachrome Corp. Model As1-C-VP-RGA) system. Prior to each adsorption experiment, the sample was outgassed at 473 K for about 12 h. Adsorption isotherms for CO_2 and CH_4 were measured at 293 K. The crystal structure of the powder was analyzed by x-ray diffraction (XRD, Scintag PAD-V diffractometer) with Cu Kα radiation.

3 RESULTS AND DISCUSSION

3.1 Silylation of MFI membranes

3.1.1 Effect of isomorphous substitution

To study the effect of isomorphous substitution of MFI membranes, Al-ZSM-5 and B-ZSM-5 membranes were prepared for silylation reaction with methydiethoxysilane. The Al-ZSM-5 membrane (A1) was prepared by in situ crystallization and had four layers with Si/Al ratio of 25 in the synthesis gel. The B-ZSM-5 membrane (B1) was prepared by secondary growth and had two layers with Si/B ratio of 12.5. Because Al or B in the zeolite framework in trivalent, the membranes should have plenty of acid sites in their H^+ form due to their low Si/Al or Si/B ratio.

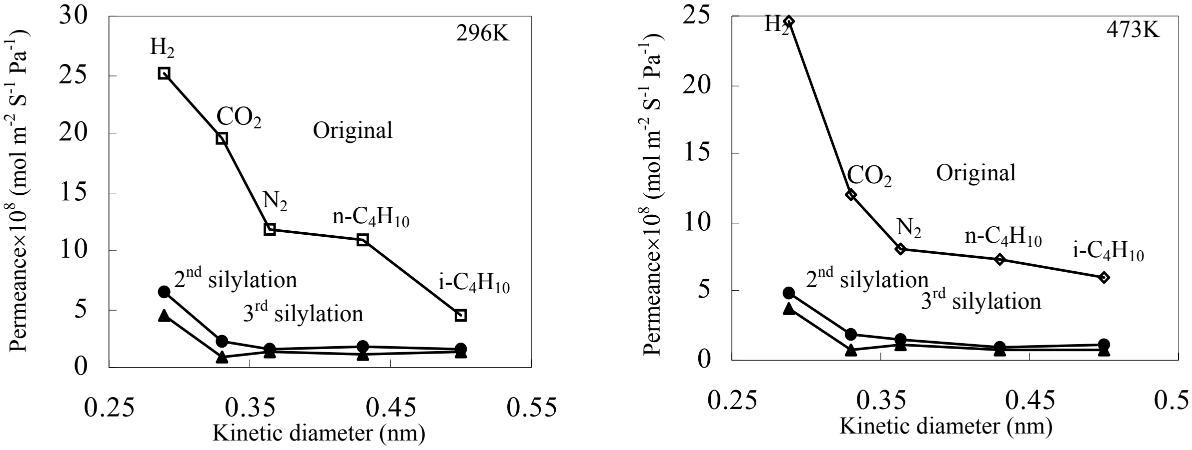

Fig.1 Single gas permeance as a function of kinetic diameter for an Al-ZSM-5 (A1) membrane before and after silylation

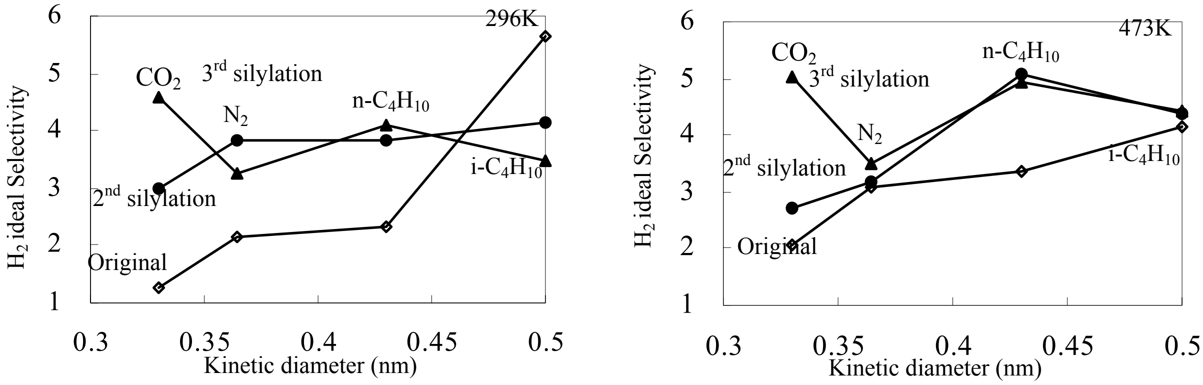

Fig.2 H_2 ideal selectivity for an Al-ZSM-5 (A1) zeolite membrane before and after silylation

The single gas permeances of different gases before and after silylation for membrane A1 are shown in Fig.1. The reduction of all the gas permeances indicates that the pore size of the membrane has been reduced. The reduction in permeance was most significant for CO_2, which became the slowest permeating molecule among those tested, although its kinetic diameter is smaller than the other gases except H_2. This trend is contrary to the majority of reports on gas transport in MFI zeolite membranes, amongst which some even reported CO_2 permeating fast than H_2 due to its strong adsorption, but in accordance to some literature on small pore zeolite membranes. Fig.2 gives the effect of silylation on the H_2 ideal selectivities over other light gases for this Al-ZSM-5 membrane. Expect for H_2/iso-butane, all the H_2/gas ideal selectivities increased after silylation. The H_2/CO_2 ideal selectivity more than doubled, suggesting that silylation is effective for light gas separations. However, big isobutane molecule was still permeating even after the 3rd silylation treatment, illustrating the inability of this method to repair large non-zeolite pores. The n-/iso-butane ideal selectivity of 1.2 at 473K for the fresh membrane also indicates that the Al-ZSM-5 membrane contained a large amount of defects and was not a good quality membrane initially.

The single gas permeances for B-ZSM-5 membrane B1 generally decreased at both 295 and 473 K as the kinetic diameter increased for the untreated membrane, as shown in Fig. 3. The only exception is CO_2, which permeates faster than H_2 at 295 K. After the membrane was silylated, the permeances of all gases except CO_2 decreased by approximately two orders of magnitude. The CO_2 permeance decreased by approximately four orders of magnitude. Thus, silylation increased the H_2/CO_2 ideal selectivity by a factor of 80 at 295 K, as shown in Fig. 4. The H_2/CO_2 ideal selectivity on the silylated membrane was 230 at 473 K; this is 120 times the selectivity of the untreated membrane. Because the CO_2 permeance was close to the detection limit of the system, the H_2/CO_2 selectivity is less accurate than the other values. The estimated errors for the H_2/CO_2 selectivities are ± 30 %. The H_2/N_2 and H_2/n-butane ideal selectivities also increased, and at 473 K the H_2/n-butane selectivity increased by a factor of 15. Note that at 473 K, i-butane permeated faster than n-butane through the silylated membrane. Thus, the H_2 selectivity relative to the other gases increased for all gases after silylation except for i-butane; the H_2/i-butane selectivity is the same or lower after silylation.

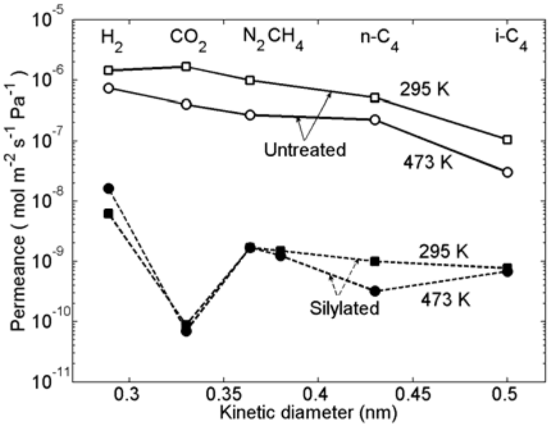

Fig. 3 Single gas permeances before and after silylation for B-ZSM-5 membrane B1 as a function of kinetic diameter at 295 K and 473 K

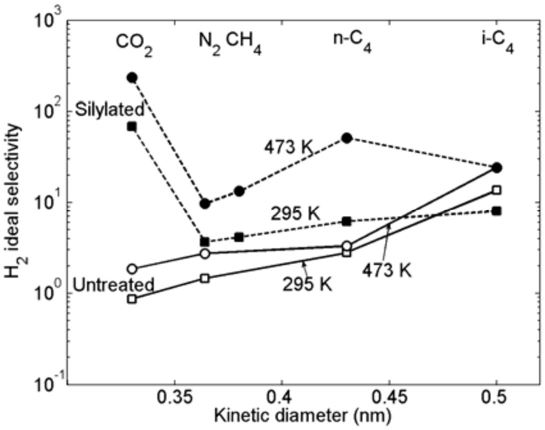

Fig. 4 H_2/gas ideal selectivity before and after silylation for B-ZSM-5 membrane B1 as a function of kinetic diameter at 295 K and 473 K

Both the Al-ZSM-5 and B-ZSM-5 membrane showed decrease in single gas permeation and increase in H_2 ideal selectivity, indicating the silylation reaction took place in both types of MFI zeolites and increased transport resistance. Boron substitution creates acid sites that should be the adsorption and reaction sites for MDES, just as the Al sites in the Al-ZSM-5 zeolite membrane, although B-ZSM-5 acid sites have lower Brönsted acid strength than Al-ZSM-5 acid sites. The silylated B-ZSM-5 membrane showed higher H_2/light gas ideal selectivity, probably because the original B-ZSM-5 membrane had better quality than the original Al-ZSM-5 indicated by higher n-/i-butane selectivities (Table 2).

Table 2. Butane permeance and ideal selectivity at 473 K and 138-kPa pressure drop for as-synthesized B-ZSM-5 membranes

Membrane number	B1	B2	B3	B4	B5	B8
Butane permeance$\times 10^8$ (mol$\cdot$m$^{-2}\cdot$s$^{-1}\cdot$Pa^{-1})	22	29	36	5.1	24	46
n-/i-butane ideal selectivity	7.4	7.2	4.0	22	14	15

To illustrate the reproducibility of the silylation experiment on B-ZSM-5 membranes, membrane B2 and B3 were also silylated. They showed similar behavior before and after silylation (not shown here). Their H_2/CO_2 ideal selectivities were lower than that of B1 after silylation, possibly because the original membrane qualities were inferior to B1, as indicated by n-/i-butane selectivity at 473 K (Table 2). The separation selectivity of H_2/CO_2, however, is only 10 at 473 K for silylated B1, much lower than the ideal selectivity.

3.1.2 Effect of initial membrane quality

The above result suggests that the initial membrane quality might be an important factor to affect the silylated membrane H_2 separation performance. To further investigate the effect of membrane quality, B-ZSM-5 membranes B4, B5, and B6 were synthesized and silylated. Hexane/2,2-dimethyl butane (C_6 isomer) separation selectivity was used to evaluate the membrane quality. The kinetic diameter of hexane is 0.43 nm, smaller than the MFI zeolite pores, while the kinetic diameter of 2,2-dimethyl butane is 0.62 nm, bigger than the MFI pores. Therefore, a good quality MFI membrane with negligible defects should be able to separate C_6 isomer with high selectivity, especially at high temperature when the adsorption effect becomes less important. Fig. 5 shows the hexane permeance and C_6 isomer separation selectivity for these three membranes. Judged by the C_6 isomer selectivity at 473 K, the membrane quality follows the order: B4 > B5 > B6, with B4 being the best membrane among them.

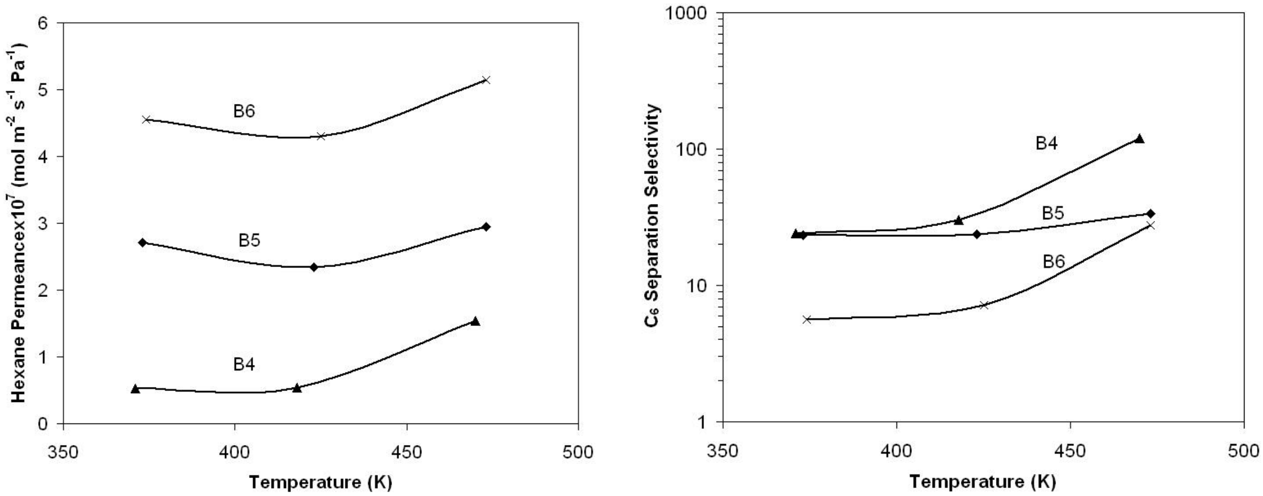

Figure 5. Hexane permeance (left) and C_6 isomer separation selectivity (right) versus temperature for B-ZSM-5 membranes B4-B6

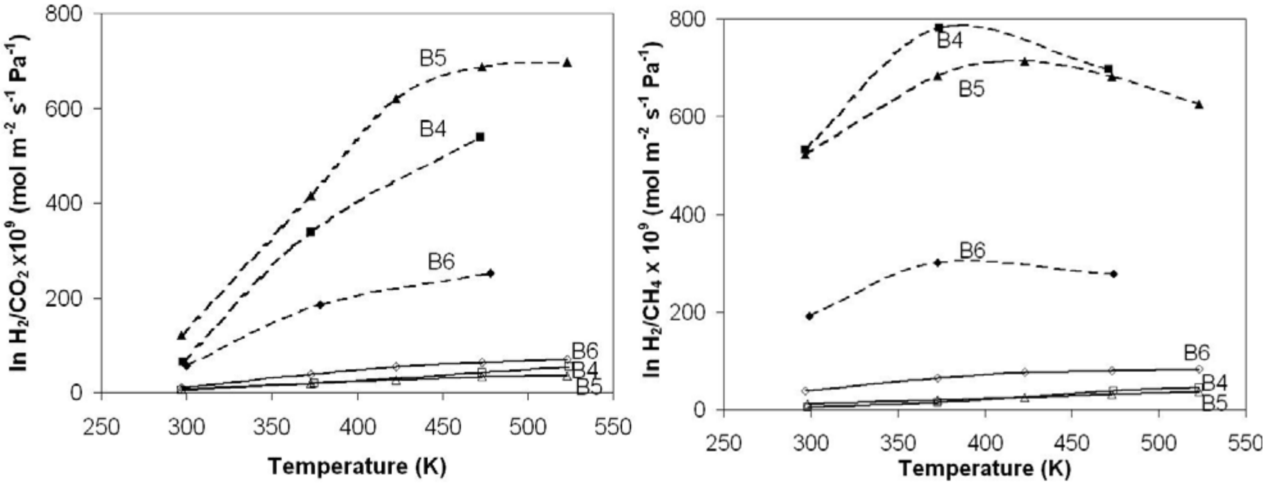

Figure 6. H_2 permeance versus temperature in the 50/50 mixture with CO_2 (left) or CH_4 (right) for B-ZSM-5 membranes B4-B6 before and after silylation (dashed line with solid symbol: before silylation; solid line with open symbol: after silylation)

The three membranes were silylated with methyldiethoxysilane and their H_2/CH_4 and H_2/CO_2 separation performance were compared before and after silylation. Fig. 6 shows the change in H_2 permeance in the mixture with CO_2 or CH_4. The H_2 permeance in the two mixtures was more than one order of magnitude lower after silylation. Although the initial H_2 permeance for these three membranes differed significantly, their H_2 permeance after silylation became similar to each other, independent of the initial H_2 permeance. Unlike the original H_2 permeance, after silylation, the H_2 permeance increased with increasing temperature. This suggests that for the original MFI membranes, H_2 permeation is more controlled by adsorption and diffusion, while for the silylated membranes, it is more controlled by activated diffusion.

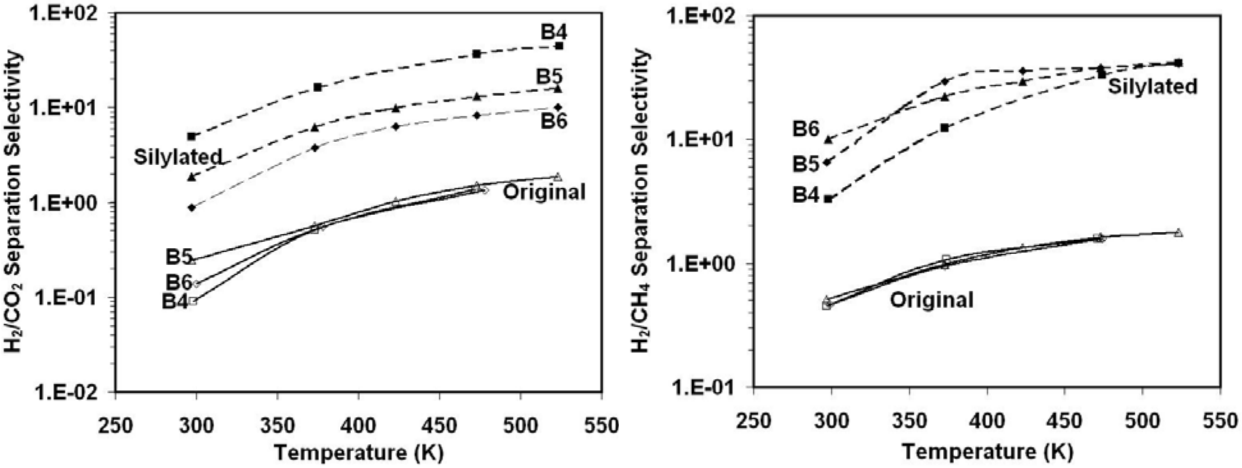

Figure 7. H_2 separation selectivity versus temperature in the 50/50 mixture with CO_2 (left) or CH_4 (right) for B-ZSM-5 membranes B4-B6 before and after silylation (dashed line with solid symbol: before silylation; solid line with open symbol: after silylation)

Although the H_2 permeances decreased significantly with silylation, the permeances of the other gases decreased more, so that the H_2/CO_2 and H_2/CH_4 separation selectivities significantly increased, as shown in Fig.7. Note that the selectivity is in logarithmic scale to make the graphs visible. The original membranes could not separate these mixtures with selectivity less one at temperatures below 373 K and slightly larger than one above 373, obviously because the MFI pores are much bigger than the light gases. At 473 K, the selectivity was still less than Knudsen selectivity (H_2/CO_2: 4.7, H_2/CH_4: 2.8). The silylated membranes could separate H_2 from CO_2 and CH_4 in the entire temperature range explored, with selectivity significantly larger than the Knudsen selectivity, especially at high temperture. This suggests that for the original MFI membranes, H_2 separation is more controlled by competitive adsorption, while for the silylated membranes, it is more controlled by differences in diffusivity. Both the H_2/CH_4 and H_2/CO_2 selectivities increased significantly as the temperature increased from 298 K to 523 K, mainly because the H_2 permeance increased with temperature. The H_2/CO_2 selectivity after silylation differs a lot with B4>B5>B6 (Fig. 7 left). This is consistent with the order of hexane isomer selectivity at 473 K (Fig.5 right: B4>B5>B6), which can be used to indicate the initial MFI membrane quality. Therefore, the H_2/CO_2 separation selectivity after silylation depends on the initial MFI membrane quality. Interestingly, H_2/CH_4 selectivity after silylation for the three membranes was similar to each other, especially at high temperatures. At 473 K, the H_2/CH_4 separation selectivity of about 42 was almost the same for the three membranes. This might be due to the fact that CH_4 (0.38 nm) is larger than CO_2 (0.33 nm). The defect sizes in the silylated MFI membranes might be mainly in between 0.33 and 0.38 nm.

Silylated membrane B4 showed high H_2 selectivities. Its H_2/CO_2 separation was studied further at high temperatures. Above 573 K, H_2 permeance in the H_2/CO_2 mixture continued to increase with temperature, but the CO_2 permeance also increased, so the selectivity leveled off (Table 3). Above 673 K, the H_2 and CO_2 reacted to form H_2O and CO; the modified B-ZSM-5 membrane catalyzed the reverse water gas shift reaction. Carbon monoxide was observed in the retentate and the permeate, but the GC could not detect water at low concentrations so the following concentrations are on a dry basis. At 723 K, the retentate contained 2% CO, and the CO concentration in the permeate was below 0.2%. The H_2 and CO_2 concentration in the permeate were 93% and 7%, respectively. At 773 K, the retentate contained 8% CO; the permeate contained 92% H_2, 7% CO_2, and 1% CO. Table 3 also gives the percent conversion of the water-gas shift reaction, hydrogen permeances, and separation selectivities at 723 and 773 K.

Table 3. H_2 permeances and separation selectivities of silylated B-ZSM-5 membrane B4 for a H_2/CO_2 mixture at high temperature

Temperature (K)	Percent Conversion	Permeance × 10^8 ($mol{\cdot}m^{-2}{\cdot}s^{-1}{\cdot}Pa^{-1}$)			Separation selectivity	
		H_2	CO_2	CO	H_2/CO_2	H_2/CO
573	-	7.3	0.15	-	48	-
623	-	8.6	0.18	-	48	-
673	-	10.2	0.22	-	47	-
723	4 %	10.5	0.23	< 0.2	46	> 48
773	15%	12.5	0.21	0.22	60	57

The stability of silylated membrane B4 was also investigated. It was stable again humidity, so that when silylated membrane B4 was stored in humid air for two months at room temperature and then heated at 523 K overnight, the permeances and selectivities at 473 K for H_2/CH_4 and H_2/CO_2 mixtures were within 2% of the values in Fig. 6 and Fig. 7. The membrane also operated at 773 K in the presence of hydrogen and water for 16 h with no degradation.

3.1.3 Effect of membrane acidity

To confirm that the silylation reaction using MDES takes place on the acid sites within the zeolite membranes, a B-ZSM-5 membrane with Si/B=100 (B7) and a silicalite-1 membrane were silylated using MDES. Membrane B7 has a lower concentration of acid sites than B1- B6 because less trivalent boron is present in the framework. Silicalite-1 is the all silicon analog of ZSM-5 without any active sites, since no trivalent Al or B is present in the framework. When the B-ZSM-5 membrane with a Si/B ratio of 100 (B7) was silylated, its H_2 permeance only decreased to half its initial value, and the H_2 selectivities relative to N_2, CO_2, and CH_4 only increased about 15% (Table 4). The H_2 permeance and separation selectivities of a silicalite-1 membrane, which does not have acid sites, did not change after silylation (permeance and selectivity change was less than 3%). This confirms that acid sites are needed for the silylation reaction with MDES, as the MDES will be pre-adsorbed there. This is also in accordance with the literature result. Therefore, the H_2 separation performance after silylation depends on the acidity of the initial MFI membranes.

Table 4. H_2 permeances and separation selectivities at 523 K before and after silylation of a B-ZSM-5 membrane with Si/B ratio of 100 (membrane B7)

Membrane	H_2 permeance in mixture $\times 10^8$ (mol·m^{-2}·s^{-1}·Pa^{-1})			Separation selectivity		
	H_2/N_2	H_2/CO_2	H_2/CH_4	H_2/N_2	H_2/CO_2	H_2/CH_4
Fresh	27	26	29	2.0	1.7	1.4
Silylated	13	13	14	2.3	1.8	1.6

3.1.4 Effect of silane precursor

Membrane B8 was synthesized using the same procedure as for membrane B1-B4 and B6, but was silylated with diluted silane (8000 ppm SiH_4 in N_2). The results, shown in Table 5, are similar to that of MDES treated membrane B1-B3: H_2 permeance dropped to 1/40 of its original value, and H_2 selectivity increased. The H_2/CO_2 ideal selectivity was also higher than 100, and the separation selectivity was lower than the ideal value. This indicates that as long as the silane precursor could penetrate into the pores of the MFI zeolites and react on the acid sites, different silane precursor would yield similar results. However, Silane is more reactive than MDES, thus the reaction is more difficult to control. It is possible that amorphous silica formed on top of the zeolite and inhibited further reaction in the zeolite pores.

Table 5. H_2 permeance and selectivities for B-ZSM-5 membrane B8 at 473 K and 138-kPa pressure drop before and after silylation.

Status	H_2 permeance$\times 10^8$ (mol·m^{-2}·s^{-1}·Pa^{-1})			Ideal selectivity		50/50 mixture separation selectivity	
	Pure H_2	In H_2/CO_2	In H_2/CH_4	H_2/CO_2	H_2/N_2	H_2/CO_2	H_2/CH_4
Original	109	77	96	1.5	2.5	1.1	1.1
Silylated	2.7	3.6	3.8	119	6.8	5.3	4.4

3.1.5 Adsorption and crystal structure study

Zeolite powders were synthesized using the same method as for synthesizing membrane B1-B4, B6, and B8 expect that surfactant was not used. The powders were also silylated twice with MDES. The original and silylated powders were mixed together with each kind of powder accounting for 50 wt%. The XRD pattern for the mixed powder is shown in Fig.8. The XRD pattern clearly shows split of peaks, indicating that the two kinds of powders have different zeolite pore sizes. Therefore, the XRD results confirm that MDES reacts in the zeolite pores of the MFI membrane. Since silane is smaller than MDES, it should also react in the MFI zeolite pores as well.

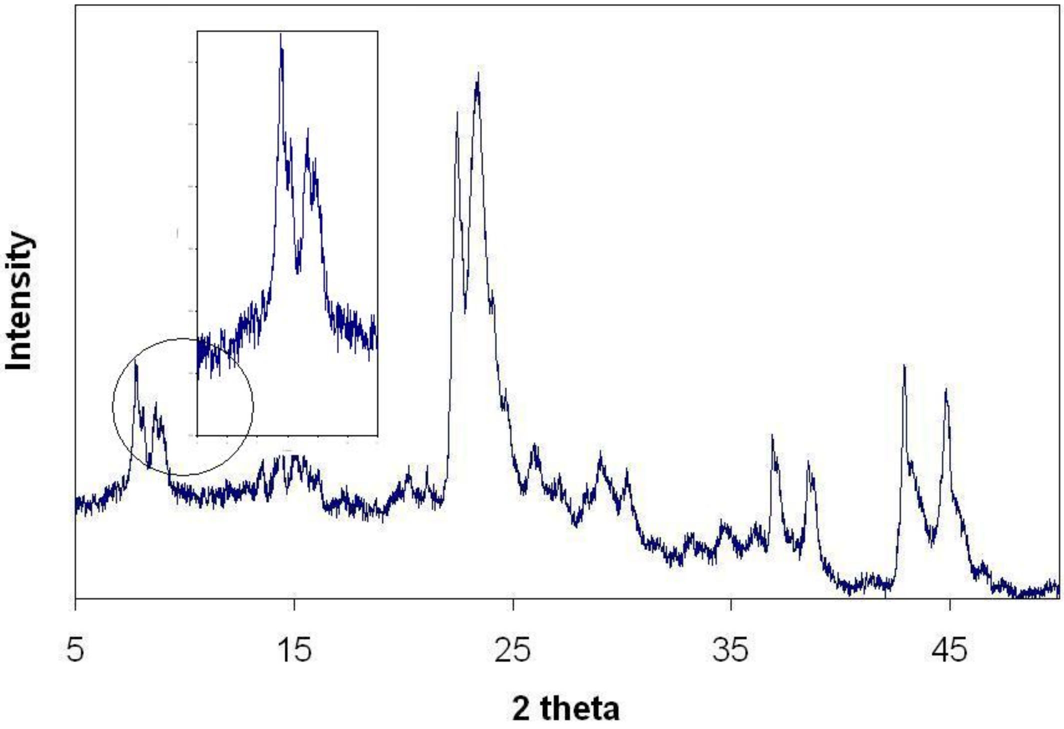

Fig. 8 XRD pattern for 50/50 mixture of as-synthesized and silylated zeolite B-ZSM-5 powders (Insert: detailed XRD pattern in 2θ range between 5 and 11)

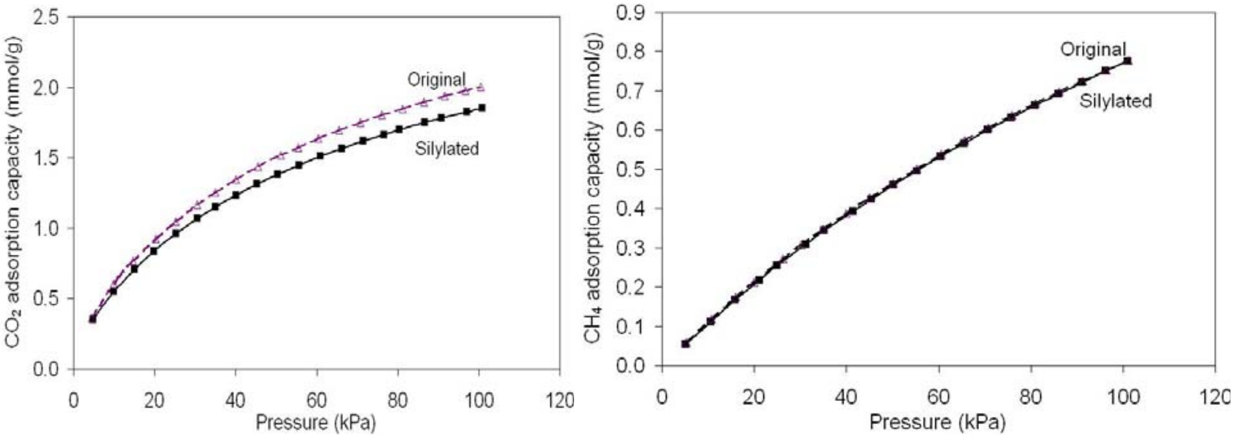

Fig. 9 Comparison of CO_2 and CH_4 adsorption isotherms at 295 K for B-ZSM-5 powders before and after silylation

The adsorption isotherms for the unsilylated and silylated B-ZSM-5 powders are shown in Fig. 9. The CO_2 adsorption amount slightly decreased after silylation, while the CH_4 adsorption amount was almost unchanged. Therefore, after silylation, the MFI zeolite pores are still big enough to adsorb CH_4. The decrease in CO_2 adsorption is probably due to the decrease in acid sites after silylation.

3.2 Silylation of CHA membranes

Two SAPO-34 membranes (S1, S2) with similar properties were prepared; their gas permeances and selectivities are shown in Table 6. The SAPO-34 is a silicoaluminophosphate and its structure is a chabazite (CHA) analog. The untreated SAPO-34 membrane S1 selectively separated H_2 from CH_4 (Fig. 10); the highest selectivity was 35, measured at 298 K. The H_2/CH_4 separation selectivity was high for the original SAPO-34 membranes because the SAPO-34 pores are almost the same size as the CH_4 kinetic diameter, which is 0.38 nm. In contrast to B-ZSM-5 membranes, silylation did not decrease H_2 permeances in mixtures for SAPO-34 membranes (Fig. 11 and Table 6). The CH_4 permeance decreased after silylation (Fig. 11), so that the H_2/CH_4 selectivity increased (Fig. 10). For clarity, the CH_4 permeance in Fig. 11 is multiplied by 20. The highest H_2/CH_4 separation selectivity for the silylated SAPO-34 membrane S1 was 59 at 298 K. As temperature increased, the H_2 permeance slightly decreased and the CH_4 permeance slightly increased, so the H_2/CH_4 separation selectivity decreased with temperature. The CH_4 permeance increased more for the silylated membrane. Thus, as shown in Fig. 10 and 11, at 525 K, silylation had no effect on permeance or selectivity. Silylation also increased the CO_2/CH_4 separation selectivity at room temperature, as shown in Table 6. The CO_2 permeance in a CO_2/CH_4 mixture decreased about 30% due to silylation.

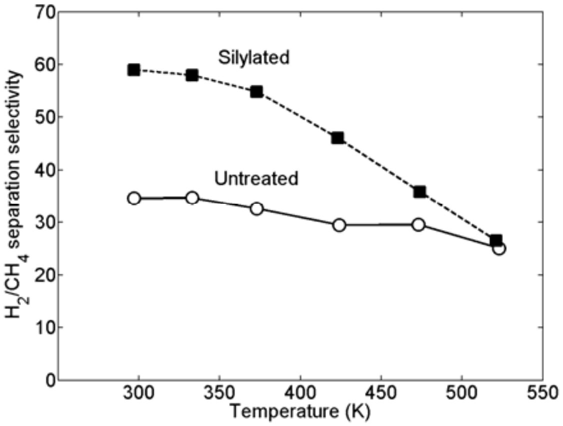

Fig. 10 H_2/CH_4 separation selectivity before and after silylation for SAPO-34 membrane S1 as a function of temperature in a 50/50 mixture of H_2/CH_4

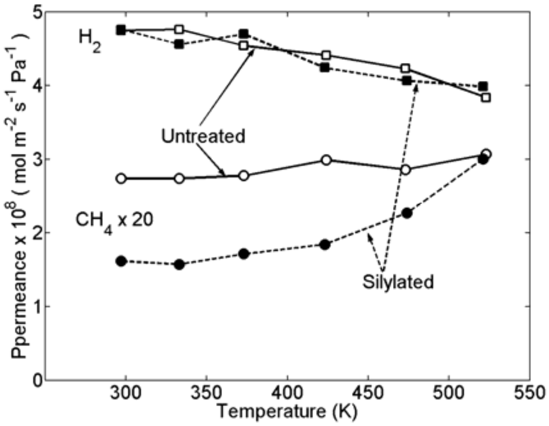

Fig. 11 H_2 and CH_4 permeances before and after silylation for SAPO-34 membrane S1 as a function of temperature in a 50/50 mixture of H_2/CH_4

Table 6. Gas permeances and separation selectivities at 298 K on SAPO-34 membranes before and after silylation

	Membrane	H_2 permeance × 10^8 ($mol \cdot m^{-2} \cdot s^{-1} \cdot Pa^{-1}$)	H_2/CH_4 selectivity	CO_2 permeance × 10^8 ($mol \cdot m^{-2} \cdot s^{-1} \cdot Pa^{-1}$)	CO_2/CH_4 selectivity
S1	Fresh	4.7	35	10	73
	Silylated	4.8	59	7.7	110
S2	Fresh	3.4	20	10	68
	Silylated	3.5	30	6.4	87

The SAPO-34 membranes had much lower selectivities for H_2/CO_2 and H_2/N_2 mixtures than for H_2/CH_4 mixtures, but the selectivities increased with temperature, as shown in Fig. 12. Silylation did not change the H_2/CO_2 separation selectivity, and it increased the H_2/N_2 separation selectivity by less than 15%. Similar to the H_2 permeance in the H_2/CH_4 mixture, the H_2 permeances in H_2/CO_2 and H_2/N_2 mixtures did not change after silylation. Similar H_2/CH_4 and H_2/CO_2 separation performance with temperature (not shown here) was seen for membrane S2 before and after silylation.

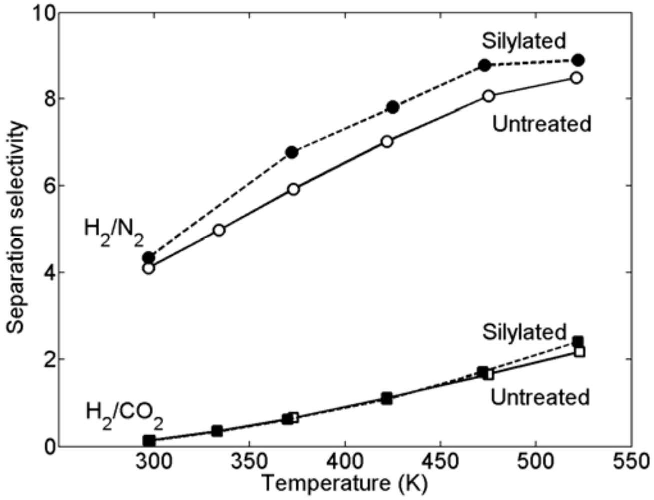

Fig. 12 Separation selectivity before and after silylation for SAPO-34 membrane S1 as a function of temperature in 50/50 mixture of H_2/CO_2 and H_2/N_2

3.3 Ion-exchange of SAPO-34 membranes

Two SAPO-34 membranes (S3, S4) were ion exchanged from the H^+ form to the metal form. Membrane S3 was exchanged with Cu^{2+} ion and membrane S4 with K^+ ion. The hydrogen permeance in H_2/CH_4 mixture was almost not affected by exchange with Cu^{2+} ion, and the H_2/CH_4 selectivity increased about 25% (Fig. 13). As for S4, however, the K^+ ion exchange decreased both its hydrogen permeance and H_2/CH_4 separation selectivity in the binary mixture (Fig. 14). This might be because the K^+ ion is too big (0.133 nm), and after K^+ exchange, the zeolite pores become so small that the transport resistance through the zeolite pores significantly increases. Therefore, a larger fraction of H_2 and CH_4 permeate through defects that are not selective. Therefore, the ion exchange of SAPO-34 membranes is not an efficient method for improving their hydrogen separation performance (as of Cu^{2+} exchange) or maybe even partially blocked the zeolite channel (as of K^+ exchange). Interestingly, both the Cu^{2+} and K^+ exchange increased the CO_2/CH_4 separation selectivity of the SAPO-34 membranes accompanied by a slight decrease in CO_2 permeance (Table 7). This might be because the CO_2 and CH_4 adsorption properties on the zeolite membranes were altered by ion exchange.

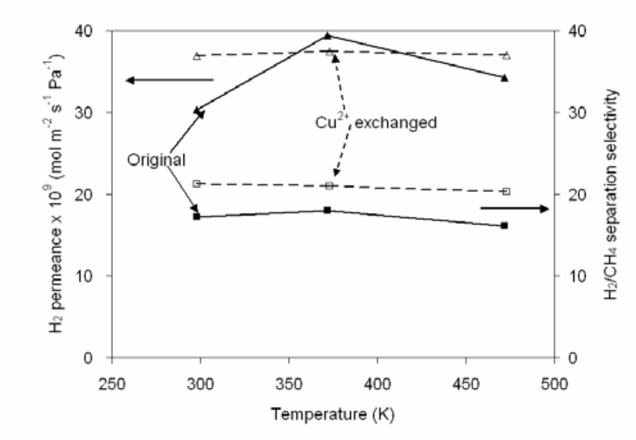

Fig. 13 H_2 permeance and separation selectivity before and after Cu^{2+} exchange for SAPO-34 membrane S3 as a function of temperature in 50/50 mixture of H_2/CH_4

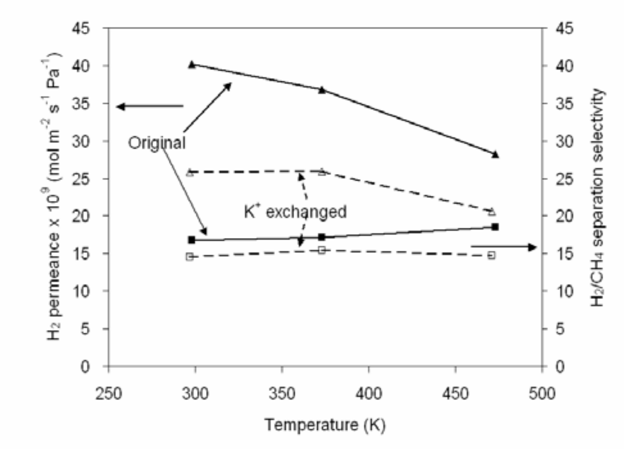

Fig. 14 H_2 permeance and separation selectivity before and after K^+ exchange for SAPO-34 membrane S4 as a function of temperature in 50/50 mixture of H_2/CH_4

Table 7. Gas permeances and separation selectivities at 298 K on SAPO-34 membranes before and after ion exchange

	Membrane	H_2 permeance× 10^8 ($mol·m^{-2}·s^{-1}·Pa^{-1}$)	H_2/CH_4 selectivity	CO_2 permeance × 10^8 ($mol·m^{-2}·s^{-1}·Pa^{-1}$)	CO_2/CH_4 selectivity
S3	Fresh	3.0	17	8.9	49
	Cu^{2+} exchanged	3.7	21	7.8	69
S4	Fresh	4.0	17	1.0	40
	K^+ exchanged	2.9	14	5.3	64

4. CONCLUSIONS

For medium pore MFI membranes, silylation using catalytic cracking of methyldiethoxysilane decreased their effective zeolite pore size and increased their H_2 separation selectivities, but H_2 permeance decreased more than an order of magnitude. The effect of silylation depends heavily on the number of acid sites within the structure, but not the strength of the acid sites. The effect of silylation also depends on the initial membrane quality. The best H_2 separation results were obtained on silylated B-ZSM-5 membranes with a Si/B ratio of 12.5 in the synthesis gel. Both the H_2 permeance and H_2/CO_2 and H_2/CH_4 separation selectivities significantly increased with temperature. The highest H_2/CO_2 and H_2/CH_4 separation selectivities were 48 and 42, respectively. The highest H_2 permeance during separations was 1.3×10^{-7} $mol·m^{-2}·s^{-1}·Pa^{-1}$. Methyldiethoxysilane and diluted silane have yielded similar results because both precursors can penetrate into the MFI pores and react on the acid sites.

For small pore CHA type SAPO-34 membranes, methyldiethoxysilane did not fit into SAPO-34 zeolite pores, but it partially blocked non-zeolite pores and increased H_2/CH_4 and CO_2/CH_4 separation selectivity while the H_2 permeance was unchanged. However, the H_2/CO_2 and H_2/N_2 selectivity was almost unchanged. The highest H_2/CH_4 separation selectivity for a SAPO membrane was 59 at 298 K.

SAPO-34 membranes in their prepared form (H^+ form) can selectively separate H_2 or CO_2 from CH_4. Ion exchange of SAPO-34 membranes from H^+ (0.0012 nm ion diameter) form to Cu^{2+} (0.072 nm) form increased the H_2/CH_4 separation selectivity possibly because decreasing the CHA pore size by exchanging H^+ to Cu^{2+} increased the transport resistance for CH_4, while smaller H_2 transport through the CHA pores was not affected. However, exchanging to K^+ (0.133 nm) form decreased H_2 permeance and H_2/CH_4 separation selectivity, indicating that the CHA pore size decreased so much by exchanging H^+ to K^+ that even H_2 had difficulty getting through CHA pores, and therefore, a higher fraction of gas flow was through non-CHA pores, which were not selective. Interestingly, both exchanges significantly increased the CO_2/CH_4 separation selectivities on SAPO-34 membranes possibly because the ion exchanges altered the SAPO-34 adsorption properties for CO_2.

5. FUTURE WORK

The silylated B-ZSM-5 membranes (Si/B=12.5 in the gel) could effectively separate H_2 from other light gases. However, H_2 permeance decreased more than an order of magnitude. Our B-ZSM-5 membranes were about 3.5 μm thick, with initial H_2 permeance about 5×10^{-7} $mol\cdot m^{-2}\cdot s^{-1}\cdot Pa^{-1}$. Thinner MFI membranes (silicalite-1) with a thickness of 0.5 μm have been reported in literature that have H_2 permeances as high as 2.2×10^{-5} $mol\cdot m^{-2}\cdot s^{-1}\cdot Pa^{-1}$ at room temperature, but their membranes do not have acid sites. Our first proposed future work is to synthesize thinner MFI membranes with large number acid sites in the structure that should have high initial H_2 permeance. Silylating such membranes might yield H_2-selective membranes with higher permeances than obtained in the current study, and that might have potential for commercial application.

As the H_2 separation performance depends on the initial membrane quality, it is desirable to use better quality membranes to start the silylation. Therefore, the membrane synthesis procedure will be improved to obtain MFI membranes with higher C_6 separation selectivity. Silylating such membranes might yield H_2-selective membranes with higher H_2 selectivities than obtained in the current study.

Although the modified MFI membranes showed promising H_2 separation properties, small pore (0.3-0.4 nm) zeolite membranes that can directly separate H_2 without the need for further modification is highly desirable. Therefore, a more interesting and challenging task is to synthesize these small pore zeolite membranes by modifying their powder preparation procedures.

We have proven that ion exchange can alter the separation properties of SAPO-34 membranes but the ions need to be carefully chosen so that they can decrease the CHA pore size to the right size desirable for separating H_2 from other light gases. Because big K^+ ion decreased the CHA pore size too much, additional ion exchange will be conducted by using smaller ions like Li^+ (0.068 nm) and Na^+ (0.098 nm) on SAPO-34 membranes. Exchange with these ions has the potential to decrease the CHA pores of SAPO-34 membranes to the size that might be appropriate size for H_2 separation.

Currently, selectivities and permeation rates were measured in binary mixtures of H_2/CO_2, H_2/CH_4 and H_2/N_2 at 138 kPa and 298-773 K. More realistic separation conditions will be explored for highly selective H_2 separation zeolite membranes, which include separation of syngas mixtures in the presence of water at elevated pressures from 100 - 2000 kPa.